ADVANCED ELECTRONIC MATERIALS Open Access
www.advelectronicmat.de

Magnetic Field Screening of 2D Materials Revealed by Magnetic Force Microscopy

Diego A. Aldave, Guillermo López-Polín, Esther Calle, Adrián Begué, Rocío Ranchal, Raúl Martínez, Cristina Bran, Enrique Burzurí, Julio Gómez-Herrero, Pablo Ares,* and Miriam Jaafar**

2D materials possess exceptional mechanical properties making them promising candidates for protecting nanostructures. However, the magnetic field screening properties of 2D materials are largely unexplored. Here it is used Magnetic Force Microscopy (MFM) to unveil the effects on the magnetic field of magnetic nanostructures when 2D materials are placed on top of them. It is demonstrated that while graphene exhibits a weak diamagnetic response due to its unique electronic structure around the Dirac point, the overall screening effect remains minimal (≈0.5% per layer). Conversely, graphene oxide (GO) and MoS_2 show negligible response to the magnetic field, making them ideal for applications where preserving the original magnetic properties is crucial. These findings suggest that 2D materials can offer effective protection while minimally affecting the underlying magnetic functionalities, important for data storage technologies and spintronics.

1. Introduction

2D materials have gained significant attention in the field of electronic nanodevices due to their unique combination of electrical, mechanical, and chemical properties.[1–3] Over the past two decades, researchers have deepened the exploration and understanding of these materials, discovering a wide range of promising characteristics.[4,5] While many of these remarkable properties of 2D materials have been extensively studied, their diamagnetic behavior remains an area that is less explored.[6] This diamagnetic nature becomes particularly relevant when considering their potential integration with magnetic nanostructures, which play a fundamental role in spintronics and data storage technologies.[7,8] The performance and reliability of these magnetic nanostructures are often affected by environmental factors.[9] This vulnerability demands the development of protective layers that can effectively safeguard these delicate structures. In this context, 2D materials emerge as promising candidates for such protective layers. Importantly, the discovery of 2D magnetic materials had a huge impact due to their potential applications in many technologies from sensing to data storage,[10] and could be easily stacked in heterostructures.[11] Of all 2D materials, graphene has the best mechanical performance, making it ideal for physically reinforcing magnetic nanostructures and improving their resistance to physical stress.[12,13]

The origin of diamagnetism in graphene can be traced back to its unique electronic structure, characterized by the presence of Dirac points and therefore a linear band dispersion around the Fermi energy. Consequently, graphene electron effective mass

D. A. Aldave, E. Calle, E. Burzurí, J. Gómez-Herrero, P. Ares
Departamento de Física de la Materia Condensada
Universidad Autónoma de Madrid
Madrid E-28049, Spain
E-mail: pablo.ares@uam.es

D. A. Aldave, E. Calle, E. Burzurí, J. Gómez-Herrero, P. Ares
Condensed Matter Physics Center (IFIMAC)
Universidad Autónoma de Madrid
Madrid E-28049, Spain

G. López-Polín
Departamento de Física de Materiales
Universidad Autónoma de Madrid
Madrid E-28049, Spain
E-mail: guillermo.lopez-polin@uam.es

A. Begué, R. Ranchal
Departamento de Física de Materiales
Facultad de Ciencias Físicas
Universidad Complutense de Madrid
Madrid E-28040, Spain

A. Begué
Facultad de Ciencias
Universidad de Zaragoza
Zaragoza E-50009, Spain

R. Martínez, M. Jaafar
Instituto de Ciencia de Materiales de Madrid (ICMM), Consejo Superior de Investigaciones Científicas (CSIC)
Madrid E-28049, Spain
E-mail: miriam.jaafar@icmm.csic.es

The ORCID identification number(s) for the author(s) of this article can be found under https://doi.org/10.1002/aelm.202400607

DOI: 10.1002/aelm.202400607

is very small resulting in a high electron mobility. Therefore, graphene under ideal conditions should present a high diamagnetic response.[14] However, imperfections, such as defects, stacking faults, and electron-phonon coupling, increase the effective mass of graphene electrons, decreasing their mobility, Fermi velocity, and opening a finite gap, all resulting in a reduction of the diamagnetism.[15,16] Despite this reduction, graphene diamagnetism would be expected to shield the magnetic field originated by an underlying magnetic structure.

On the other hand, graphene oxide (GO), a derivative of graphene, possesses oxygen-containing functional groups on its surface. These functional groups produce modifications on their electronic structure, increasing the effective mass of the charge carriers, opening a band gap, and therefore reducing its diamagnetism. However, their magnetic properties are not fully understood, with reports suggesting ferromagnetism in graphene oxide,[17,18] paramagnetism or even weak diamagnetism at room temperature.[19] As a result, we expect a significantly different behavior of the magnetic field when covering the magnetic structures with graphene and with GO. Additionally, the well-documented mechanical properties of GO, similar to graphene,[7] are promising for offering physical protection to the underlying substrate while minimizing interference with its magnetic signature.

Similarly, MoS_2, a semiconducting 2D material, also exhibits minimal diamagnetism.[20] Its layered structure and semiconducting nature make it a potential candidate for multiple applications, including its integration in 2D transistors.[21] and its combination with other technologically relevant materials such as ferroelectrics,[22] and its negligible diamagnetic response could be advantageous in situations where any magnetic field disruption needs to be minimized.

Our work explores the ability of these 2D materials to shield the magnetic signal from different underlying magnetic structures. Our findings aim to clarify the potential of 2D materials in enhancing the performance and reliability of magnetic nanostructures, paving the way for advancements in spintronics and data storage technologies.

2. Results and Discussion

2.1. Diamagnetic Response of 2D Materials

We deposited the 2D materials on top of several kinds of substrates with different magnetic anisotropies, ranging from in-plane to out-of-plane. Magnetic anisotropy refers to the preference of a material's magnetization to align along a specific direction. This easy axis for magnetization depends on the material's crystal structure and electronic properties. Samples with in-plane anisotropy are those in which magnetization prefers to lie within the plane of the material (parallel to the surface), while samples with out-of-plane anisotropy are those in which the magnetization prefers to lie perpendicular to the plane of the material (pointing out of the surface). The type of anisotropy present in a material affects its magnetic properties and behavior. For example, materials with strong out-of-plane anisotropy are desirable for perpendicular magnetic recording (used in magnetic hard drives),[23] spintronic devices such as Magnetic Tunnel Junctions,[24] Spin-Transfer Torque (STT)[25] memories or energy harvesting devices based on thermomagnetic effects.[7] On the other hand, samples with in-plane anisotropy are used for sensors[26] or magnetic memory devices.[27]

First, we used commercially available magnetic hard disks where the magnetization is in-plane. Second, we also employed Magnetic Force Microscopy (MFM) chip cantilevers as substrates where the magnetization corresponds to out-of-plane stripes. The third type of substrates are electrodeposited $Ni_{90}Fe_{10}$ films, a metallic alloy with relevant magnetoelastic properties where out-of-plane stripe domains are visible in MFM images.[28] Finally, we used SiO_2 substrates with ferromagnetic cylindrical nanowires deposited on the surface.

We transferred few-layer graphene (FLG) and MoS_2 flakes by an all-dry deterministic transfer using polydimethylsiloxane (PDMS).[29] (**Figure 1a–d**), and GO flakes by drop casting (Figure 1e,f) onto these substrates. For the nanowires, we spin-coated them onto SiO_2 substrates and then covered them by deterministic transfer of FLG flakes in some cases and drop casting of GO flakes in others.

We used the MFM technique to study the shielding of the magnetic fields generated by the different substrates mentioned above due to the presence of 2D materials on their surface. MFM is a non-destructive technique that can be used to study a wide variety of magnetic materials. All measurements were performed in amplitude modulation (AM) mode, so that the magnetic signal was obtained from the phase shift or frequency shift (when a Phase Lock Loop [PLL] was activated). In this mode, the interaction between the MFM tip and the underlying magnetic domains leads to a shift in the cantilever's oscillation frequency and phase. This frequency (phase) shift is directly proportional to the strength of the magnetic field gradient experienced by the tip, allowing variations in magnetic signal strength to be quantified. Due to the different electronic nature of the studied materials, electrostatic compensation can play an important role. Therefore, the combination of Kelvin Probe Force Microscopy (KPFM) with MFM[30,31] was used to avoid any possible influence of electrostatics. A standard two-step MFM measurement approach was adopted to neglect any short-range (van der Waals) interaction between the MFM tip and the surface. In the first step, the topography of both the bare surface and the surface covered with 2D materials was acquired in the AM operation mode. This step provided a detailed topography of the surface, including the thickness of the deposited 2D layers (see for instance **Figure 2a**). The second step involved a retrace pass performed at a defined lift height above the surface. This lift height was calculated considering the height of both bare and covered surfaces to ensure that short-range interactions were negligible. In this way, this approach enabled the acquisition of the true magnetic signal from the frequency or the phase channel. By mapping the frequency (phase) shift values obtained during the retrace pass, an image representing the distribution of the magnetic signal across the sample surface was generated.

C. Bran
Instituto de Nanociencia y Materiales de Aragón (INMA-CSIC)
Universidad de Zaragoza
Zaragoza E-50009, Spain

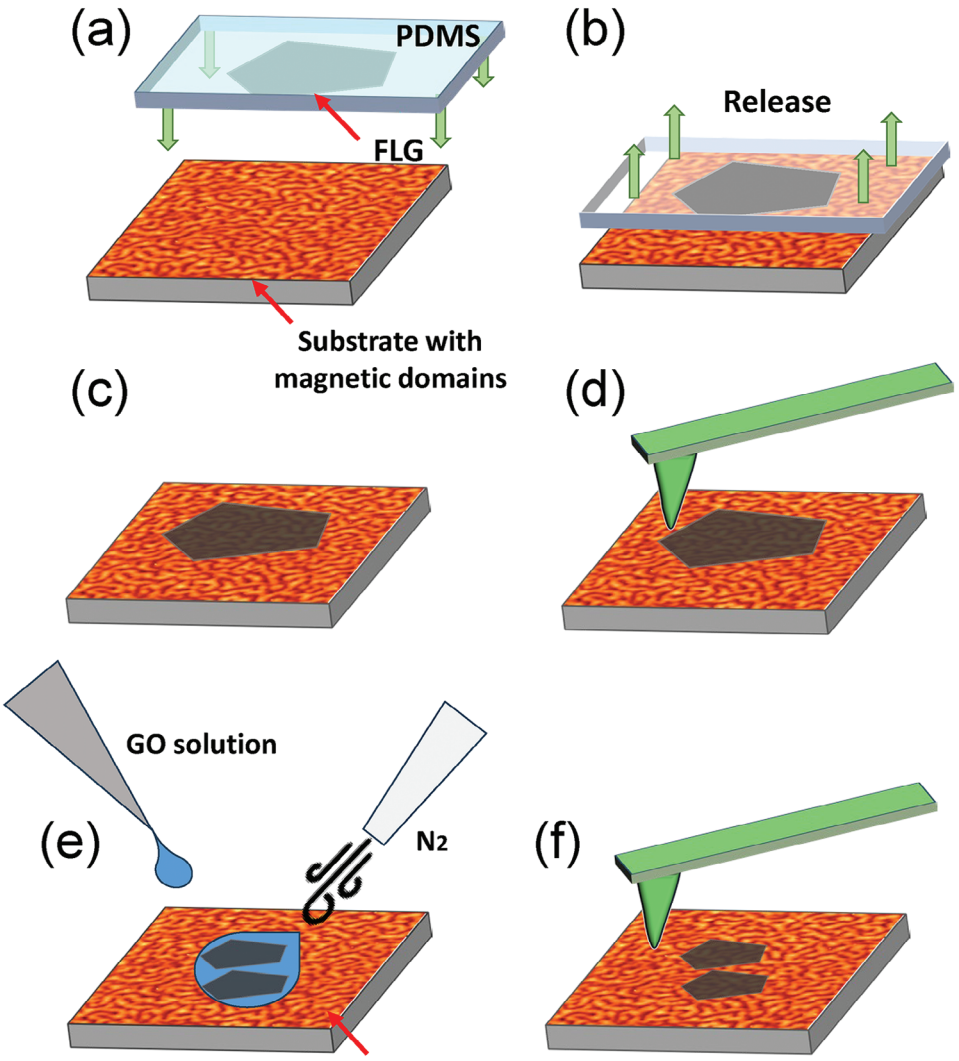

Figure 1. Scheme of the procedure used to prepare and measure the samples. a)-d) describe the PDMS based transfer method used to prepare FLG and MoS_2 flakes on substrates with magnetic domains and the MFM measurements. e,f) show the drop casting method used for preparing the GO flakes on the different substrates and the MFM measurements on these kinds of samples.

The second scan can be performed in different ways. On one side, the topography profile acquired in the first image can be repeated. This method would not be appropriate in this experiment since when we are measuring the 2D-covered materials we would be further away from the magnetic material than in the uncovered areas. The correct method for this study is to set the second trace to an average plane or profile in such a way that the tip is always at the same distance from the ferromagnetic material, regardless of whether it is covered or not. In the case of samples with a high number of layers, this explains the ranges used, between 20 and 350 nm, to avoid interactions with the top parts of the covering 2D flakes.

Furthermore, we also used a spectroscopy mode (frequency shift spectroscopy) to measure how the frequency shift varied as a function of the distance at each point of the topography (see Supporting Material S1 in the Supporting Information, SI). Knowing the thickness of the flakes, we can identify the frequency shift at the same distance from the substrate at each point. This technique provides results consistent with the method described above.

While MFM possesses the resolution to analyze such small samples, it inherently cannot directly quantify the intrinsic susceptibility of the material. Therefore, the quantification of the magnetic signal change relied on the analysis of the RMS amplitude of the frequency shift oscillations within designated regions of interest of the same area (see Supporting Material S2 in the Supporting Information SI). These regions were carefully chosen to encompass zones both inside and outside the deposited 2D material flakes. By comparing the RMS amplitude values from these regions, we could assess the relative decrease in magnetic signal strength caused by the presence of the 2D material layer. This procedure was repeated for samples with different types of 2D materials (FLG, GO, and MoS_2) and varying their thicknesses, allowing us to evaluate the impact of these materials on the magnetic properties of the underlying nanostructures. In addition, the use of average profiles has been used to quantify the

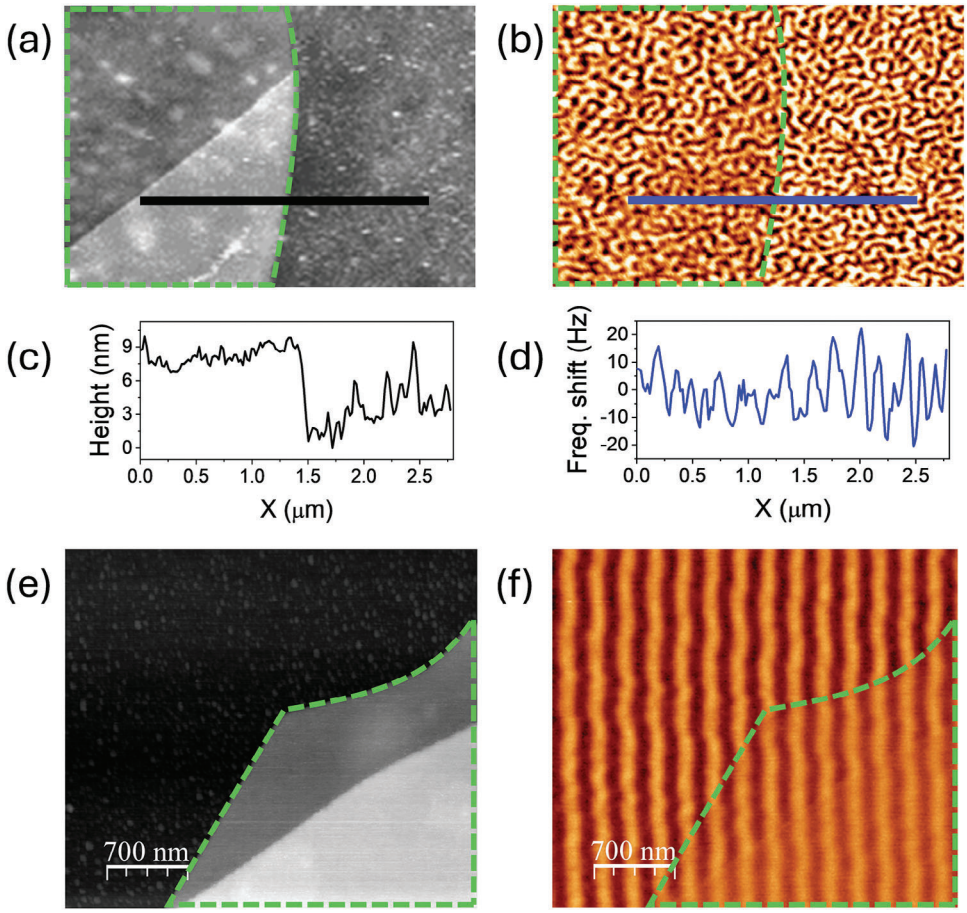

Figure 2. a) AFM topography and magnetic signal b) of a FLG transferred to an MFM chip cantilever with wormlike magnetic domains. The profiles c) and d) show that the magnetic signal is reduced on the FLG. Topography e) and magnetic signal f) of a FLG covering magnetic domains of a magnetic hard disk. In all the cases, the edges of the FLG flakes are outlined with dashed green lines for clarity.

screening effect of the 2D materials in selected areas (see Supporting Material S3 in the Supporting Information SI).

A representative MFM measurement of the magnetic signal of an FLG flake partially covering a magnetic substrate is shown in Figure 2. As the profile reveals, there is a subtle decrease in the magnetic signal intensity for regions covered with FLG (Figure 2d). This decrease corresponds to a reduction of ≈0.5% per layer of graphene, suggesting a minimal shielding effect due to this material. This observation aligns with theoretical predictions for single-layer graphene, which exhibits a weak diamagnetism due to its unique band structure around the Dirac points.[1]

Similarly, **Figure 3** shows representative magnetic signal images of GO and MoS_2 flakes covering part of a magnetic hard disk and a $Ni_{90}Fe_{10}$ film, respectively. Contrary to the case of FLG, GO and MoS_2 exhibited negligible diamagnetic response. This aligns with the presence of various functional groups in GO,[32] and the presence of S-vacancies and grain boundaries in MoS_2,[20,33] which introduce unpaired electrons into the electronic structure of these materials. These electrons interact with the magnetic field of the substrate, resulting in localized magnetic moments that contribute to the reduction or suppression of any intrinsic diamagnetism in both materials.

The images presented in Figures 2,3 are part of a broader dataset obtained from various 2D materials (GO, FLG, and MoS_2) deposited on a range of substrates. While only four specific examples are shown for illustrative purposes (two for FLG, one for GO, and one for MoS_2), similar trends were observed across all material-substrate combinations. **Figure 4** summarizes the MFM measurements on the different samples, plotting the normalized MFM magnetic signal as a function of the number of layers of the different 2D materials.

On the one hand, no relevant differences in the magnetic signal are observed for either MOS_2 or GO. This may be a consequence of the rising population of unpaired electrons with the number of layers in both materials. Each layer may introduce additional features (functional groups, vacancies or grain boundaries) that disrupt the structure of these materials, minimizing any possible diamagnetic response, as discussed above. On the other hand, our results reveal an intrinsic shielding effect due to the presence of FLG. The effect is quantified by the decrease of the MFM signal with the increasing number of layers. By analyzing an hBN/FLG heterostructure we have confirmed that the origin of this screening comes from the nature of the graphene itself and not from the FLG interaction with the magnetic substrates (see Supporting Material S4 in the Supporting

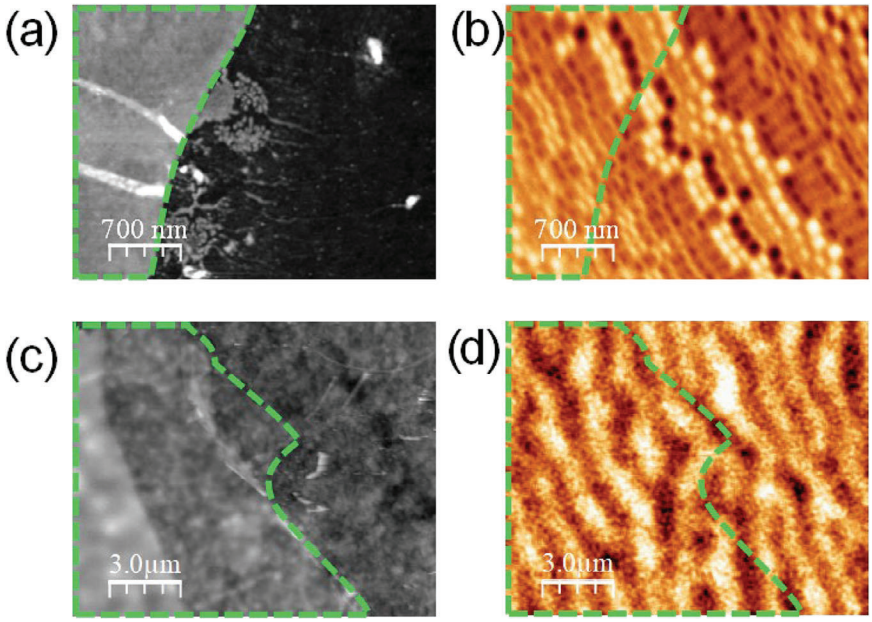

Figure 3. a) AFM topography and b) magnetic signal of GO (height ≈6.5 nm) covering a magnetic hard disk with in-plane magnetic domains. c) and d) Similar to a) and b), but now there is MoS_2 (terrace heights ≈7, 15 and 26.5 nm) on a $Ni_{90}Fe_{10}$ film. No significant difference can be observed between covered and uncovered areas. In all the cases, the edges of the flakes are outlined with dashed green lines for clarity.

Information SI). The variability in the data aligns with the findings presented in the study by B. Semenenko and P.D. Esquinazi on diamagnetism in bulk graphite.[16] There it was proposed that the dominant diamagnetic contribution in bulk graphite arises from highly conducting 2D interfaces within the structure, rather than from the intrinsic properties of the ideal graphene layers. These interfaces, arising from defects, impurities or variations in stacking order, can introduce inhomogeneities in the diamagnetic response across the FLG surface. In addition, it was emphasized the importance of sample size and thickness in isolating the intrinsic diamagnetic response, suggesting measuring thinner and smaller graphite samples (down to 10 nm thickness and 1 μm^2 area) to minimize the influence of these interfaces. The observed variability in our FLG measurements could be attributed to the influence of such interfaces present within the flakes, especially for those whose thicknesses and sizes are above the suggested values for which the uncertainty is significantly higher. Another source of variability in our measurements is the inherent variation in the magnetic domain structure across the sample surface. Doping level, a factor beyond our experimental control, is also potentially influencing magnetic shielding.[14] However, the crucial observation is the systematic decrease in the magnetic signal with graphene and the complete absence of any change with GO and MoS_2. In the first case, the findings highlight a weak diamagnetic behavior of graphene. Nevertheless, the combined effect of n layers of this material would attenuate the magnetic field by a factor $(1 - r)^n$, where r is the shielding factor of a single layer of graphene (0.5%, as mentioned above). Therefore, graphene emerges as a potentially attractive material for applications where partial modulation or control of stray magnetic fields is desirable, such as in spintronic devices with intricate magnetic field interactions.[34] As for the second case, the minimal influence of GO and MoS_2 on the magnetic signal highlights their potential as protective layers for magnetic nanostructures, as they offer minimal magnetic field disruption while potentially mitigating environmental degradation.

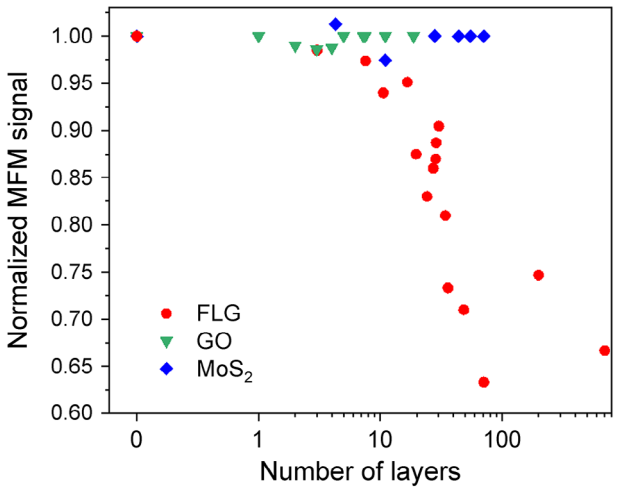

Figure 4. Magnetic field screening quantified by the decrease of the MFM signal for regions covered by FLG, GO, and MoS_2 as a function of the number of layers.

2.2. Impact on Magnetic Nanostructures

The previous results demonstrate the influence of different 2D materials on thin-film-type magnetic samples with varying magnetic anisotropies. However, in spintronic devices and other electronic devices not only thin films but also 3D materials are

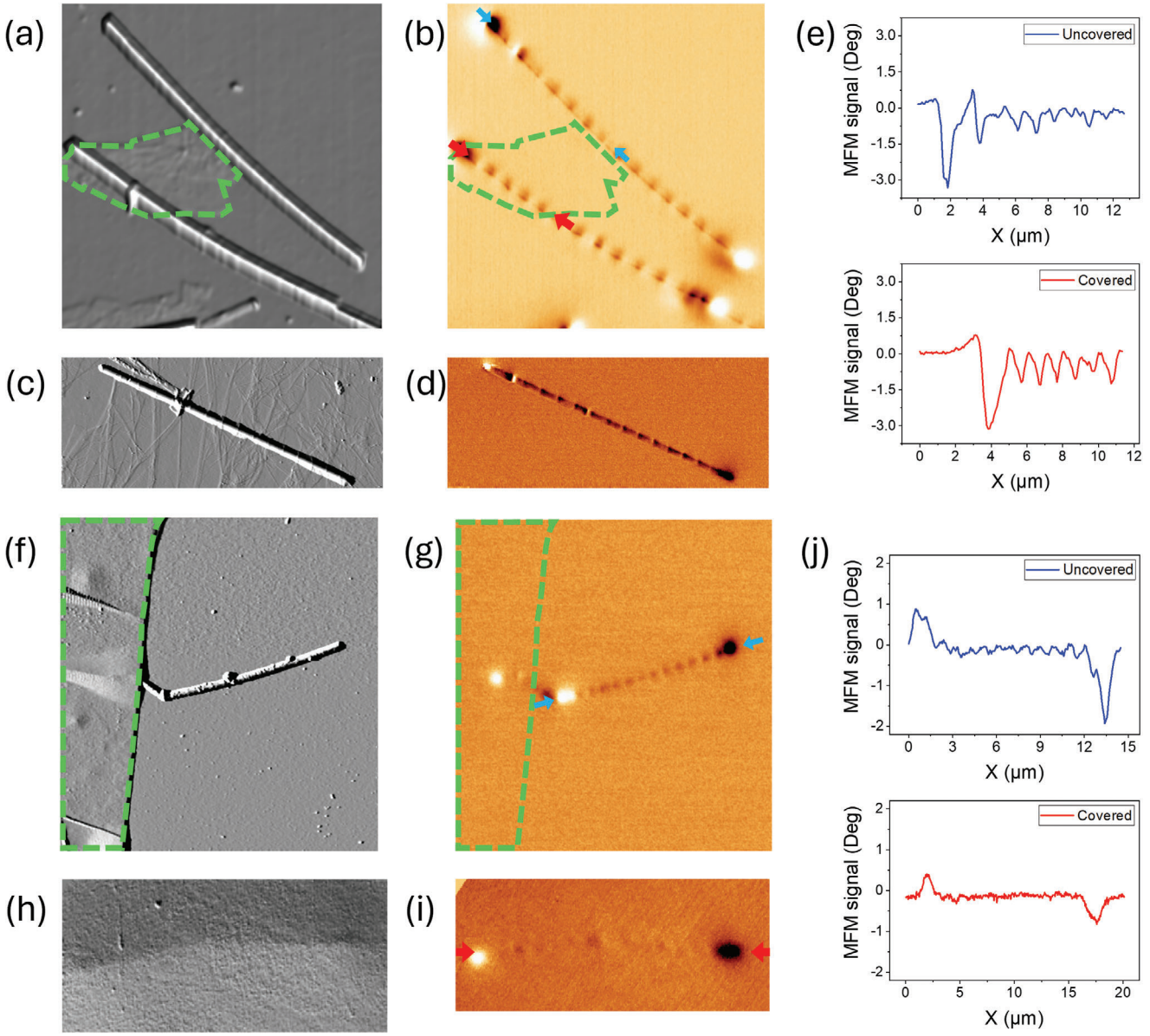

Figure 5. Topographic and magnetic images of individual NWs covered by GO and FLG. a) AFM topography of several NWs showing both uncovered and covered with GO. b) Corresponding MFM image of a). The dashed green lines outline the edge of the GO flake. c) AFM topography of a single NW covered with GO and d) its corresponding MFM image. e) Profiles along the MFM signal of an uncovered (top) and covered NW (bottom) with GO, showing no appreciable changes in the amplitude of the signals. f) AFM topography of several NWs showing both uncovered and covered with FLG. g) Corresponding MFM image of f).The dashed green lines outline the edge of the FLG flake. h) AFM topography of a single NW covered with FLG and i) its corresponding MFM image. j) Profiles along the MFM signal of an uncovered (top) and covered NW (bottom) with FLG, showing a visible decrease in the amplitude of the signal in the covered NW. In all cases, the blue and red arrows indicate the edges of the blue and red profiles in the MFM images.

used.[35] These materials may be susceptible to oxidation, local heating, or strain. As a result, combining them with different 2D materials that may act as protective or activating layers could be beneficial.

Figure 5 shows a summary of the most significant results of combining FLG and GO with modulated magnetic nanowires. The composition of the NWs alloy is $Fe_{28}Co_{67}Cu_5$ (hereafter referred to as the FeCoCu nanowires). As expected, due to the shape anisotropy, the strong dark-white magnetic contrast confirms the overall axial magnetization in the nanowires. The intermediate dark-bright pattern conversely evidences the presence of magnetic charges accumulated at the periodically imprinted geometrical modulations along the length of the nanowires.

When GO was deposited on magnetic nanowires, it did not screen nor alter the magnetic contrast (Figure 5a–e). This suggests that GO can effectively act as a protective layer, preventing oxidation or corrosion of the underlying magnetic nanowires without altering their intrinsic magnetic properties, in agreement with our previous observations on thin films (Figures 3 and 4). This characteristic makes GO a promising

candidate for encapsulating magnetic nanowires used in data storage devices, where environmental factors can significantly impact performance and reliability.[36,37]

FLG, on the other hand, exhibited a slight shielding effect on the magnetic signal of nanowires. As can be seen in the profiles (Figure 5f–j), the intermediate contrast that appears due to the accumulated magnetic charges in the FeCo/Cu interlayers disappears completely in the NWs covered by the FLG flakes. On the other hand, the bright/dark contrast at the ends of the NW decreases gradually due to the reduction of the magnetostatic interaction between the tip and the sample thanks to the graphene shielding.

3. Conclusions

This work explores the capability of different 2D materials to screen the magnetic signal from different underlying magnetic structures. We employed MFM to investigate the interaction between graphene (FLG), graphene oxide (GO), and MoS_2 with prepatterned magnetic domains on commercially available magnetic hard disks, MFM chip cantilevers, thin films with stripe domains, and magnetic nanowires.

Our findings suggest that FLG exhibits a weak diamagnetic response, consistent with experimental results and theoretical predictions for single-layer graphene.[38] This characteristic suggests its potential for applications where minimal magnetic field modulation is desired. Other properties of graphene, such as its high Young's modulus, mechanical strength, and the relative ease of fabrication, allow for better integration into new-generation devices while preventing mechanical damage to the heterostructures in which it is present. Moreover, its exceptional thermal conductivity would allow efficient heat dissipation during device operation, which can be critical in spintronic and data storage devices where high-speed operation can lead to significant Joule heating. Conversely, GO and MoS_2 display negligible diamagnetism, making them promising candidates as a protective layer due to their minimal magnetic field disruption and potential for mitigating environmental degradation. In addition, these materials could be combined in magnetic device architectures with 2D ferromagnets, such as Fe_3GeTe_2 or Fe_3GaTe_2, which present long-range magnetic order along the plane and the weak interlayer forces between monolayers.[39] This will help to increase integration as well as reduce power consumption.

In the case of magnetic nanowires, the gradual decrease of the bright/dark contrast at the ends of the NWs might be beneficial for specific applications where controlled magnetic field interactions with nearby elements are crucial. For instance, FLG spacers could be strategically placed in magnetic nanowire devices to tailor their response to external magnetic fields. Another advantage of the FLG combination with magnetic nanowires would be its use as an electrode for magnetotransport measurements.

Further investigations would imply the manipulation of the diamagnetic response of graphene through a gate voltage to dope the system. Utilizing controlled doping methods and complementary characterization techniques would help understanding this phenomenon, although these challenging measurements are out of the scope of the present work.

Overall, this work demonstrates the potential of 2D materials like FLG, GO, and MoS_2 for various applications in magnetic device architectures. By harnessing their unique properties and exploring advanced manipulation techniques, it can pave the way for the development of novel magnetic devices with enhanced functionality and performance for future technological advancements.

4. Experimental Section

Sample Preparation: Commercially available magnetic hard disks were employed as substrates due to their well-defined and readily available magnetic recording domains. Additionally, MFM chip cantilevers with prepatterned magnetic domains were utilized to provide a controlled and easily characterizable platform for MFM measurements. Finally, two more representative samples were analysed: a 1 µm thick $Ni_{10}Fe_{90}$ thin film with stripe domains[28,40] and modulated FeCoCu individual nanowires.[41]

For the preparation of graphene and MoS_2 flakes, it was employed the well-established polydimethylsiloxane (PDMS) transfer method. High-quality natural graphite was mechanically exfoliated to yield FLG flakes. These flakes were then carefully transferred onto the desired substrate (magnetic hard disk, MFM chip cantilever, thin film with stripe domains, and nanowires) using PDMS stamps. The PDMS stamp acts as a temporary carrier, allowing for the controlled placement of the flakes on the target surface.

GO flakes were prepared via chemical exfoliation of graphite, oxidizing the graphite using the Hummers method[42] and dispersing the graphite oxide in water.[43] Two distinct approaches were employed to achieve different GO layer thicknesses:

- For thin GO layers, a controlled amount of the GO solution was carefully placed as a drop onto the substrate. This drop was allowed to remain on the surface for several minutes, allowing for partial evaporation of the solvent and some degree of self-assembly of the GO flakes. The process was then terminated by gently blowing the remaining solvent with a stream of nitrogen gas. This technique typically results in the formation of relatively thin and uniform GO layers.

- For thicker GO layers, a similar approach was employed, but the GO solution drop was left undisturbed on the substrate. This allowed for complete evaporation of the solvent at ambient conditions. As the solvent evaporates, the GO flakes tend to concentrate and self-assemble, leading to the formation of thicker GO films on the substrate.

Magnetic Force Microscopy (MFM): The interaction between the 2D materials and the underlying magnetic domains was investigated using Magnetic Force Microscopy. It was employed a custom-built AFM equipped with commercially available MFM tips from Nanosensors (PPP-MFMR). The specific tip material and coating (e.g., CoCr-coated silicon tip) were chosen for their sensitivity to magnetic field gradients. The AFM's operation was controlled by Dulcinea Electronics, a dedicated AFM control system, and the data acquisition and analysis were performed using the WSxM software,[44,45] a widely used platform for AFM data processing.

MFM measurements were conducted at room temperature in dynamic AM mode. This mode is a non-contact imaging technique where the MFM tip oscillates at its resonant frequency while being maintained at a constant average distance (set point) above the sample surface. The force modulation parameters, such as the set point and the frequency modulation amplitude, were carefully optimized for each sample type to achieve high-resolution imaging of the magnetic domain features. Depending on the experiment, the magnetic signal was measured in frequency shift (if a PLL was used) or in phase shift.

The WSxM software served as the primary tool for analyzing the MFM data. This software offers various functionalities for image processing, data analysis, and visualization. WSxM allows to calculate various statistical parameters like the average, standard deviation, and distribution of the frequency shift values within designated regions of interest. By comparing these statistical values for areas with and without 2D material coverage, the average decrease in magnetic signal strength can be quantified and the variability of this effect across different regions of the sample assessed.

Supporting Information

Supporting Information is available from the Wiley Online Library or from the author.

Acknowledgements

This research was funded by the Spanish Ministry of Science, Innovation and Universities & the State Research Agency MICIU/AEI/10.13039/501100011033, grant numbers PID2021-122980OA-C53, PID2021-122980OB-C51 (AEI/FEDER), PID2021-123295NB-I00, PID2022-138908NB-C32, PID2022-142331NB-I00, TED2021-130957B-C55, TED2021-132219A-I00, CNS2023-143713, Ramón y Cajal fellowship RYC2020-030302-I, and "María de Maeztu" Programme for Units of Excellence in R&D (CEX2023-001316-M) A. B. would like to acknowledge the funding received from the Ministry of Universities and the European Union-Next Generation for the Margarita Salas fellowship. Special mention should be made of the Fundación Max Mazin, which in collaboration with the CSIC, has made it possible for R. M. to participate in this project.

Conflict of Interest

The authors declare no conflict of interest.

Data Availability Statement

The data that support the findings of this study are available from the corresponding author upon reasonable request.

Keywords

2D materials, graphene materials, magnetic field screening, magnetic force microscopy, MoS_2

Received: August 2, 2024
Revised: October 1, 2024
Published online:

[1] A. H. Castro Neto, F. Guinea, N. M. Peres, K. S. Novoselov, A. K. Geim, *Rev. Mod. Phys.* **2009**, *81*, 109.
[2] G. Lopez-Polin, C. Gomez-Navarro, J. Gomez-Herrero, *Nano Mater. Sci.* **2022**, *4*, 18.
[3] R. S. Sundaram, C. Gómez-Navarro, K. Balasubramanian, M. Burghard, K. Kern, *Adv. Mater.* **2008**, *20*, 3050.
[4] R. Mas-Balleste, C. Gomez-Navarro, J. Gomez-Herrero, F. Zamora, *Nanoscale* **2011**, *3*, 20.
[5] P. Ares, K. S. Novoselov, *Nano Mater. Sci.* **2022**, *4*, 3.
[6] E. Marchiori, L. Ceccarelli, N. Rossi, L. Lorenzelli, C. L. Degen, M. Poggio, *Nat. Rev. Phys.* **2022**, *4*, 49.
[7] G. Lopez-Polin, H. Aramberri, J. Marques-Marchan, B. I. Weintrub, K. I. Bolotin, J. I. Cerdá, A. Asenjo, *ACS Appl. Energy Mater.* **2022**.
[8] S. P. Gubin, *Magnetic nanoparticles*, John Wiley & Sons, Hoboken, N.J., US **2009**.
[9] A. Baron, D. Szewieczek, G. Nawrat, *Electrochim. Acta* **2007**, *52*, 5690.
[10] H. Li, S. Ruan, Y. J. Zeng, *Adv. Mater.* **2019**, *31*, 1900065.
[11] K. S. Novoselov, A. Mishchenko, A. Carvalho, A. C. Neto, *Science* **2016**, *353*, aac9439.
[12] G. Lopez-Polin, J. Gomez-Herrero, C. Gómez-Navarro, *Nano Lett.* **2015**, *15*, 2050.
[13] C. Lee, X. Wei, J. W. Kysar, J. Hone, *Science* **2008**, *321*, 385.
[14] J. Vallejo Bustamante, N. Wu, C. Fermon, M. Pannetier-Lecoeur, T. Wakamura, K. Watanabe, T. Taniguchi, T. Pellegrin, A. Bernard, S. Daddinounou, *Science* **2021**, *374*, 1399.
[15] M. Koshino, T. Ando, *Phys. Rev. B Condens. Matter* **2007**, *75*, 235333.
[16] B. Semenenko, P. D. Esquinazi, *Magnetochemistry* **2018**, *4*, 52.
[17] S. Qin, X. Guo, Y. Cao, Z. Ni, Q. Xu, *Carbon* **2014**, *78*, 559.
[18] A. Sinha, A. Ali, A. D. Thakur, *Mater. Today Proc.* **2021**, *46*, 6230.
[19] X. Zhang, G. Li, Q. Li, M. Shaikh, Z. Li, *Results Phys.* **2021**, *26*, 104407.
[20] S. Tongay, S. S. Varnoosfaderani, B. R. Appleton, J. Wu, A. F. Hebard, *Appl. Phys. Lett.* **2012**, 101.
[21] M. Chhowalla, D. Jena, H. Zhang, *Nat. Rev. Mater.* **2016**, *1*, 16052.
[22] M. O. Ramírez, P. Molina, D. Hernández-Pinilla, G. López-Polín, P. Ares, L. Lozano-Martín, H. Yan, Y. Wang, S. Sarkar, J. H. Al Shuhaib, *Laser Photonics Rev.* **2024**, *18*, 2300817.
[23] V. Parekh, E. Chunsheng, D. Smith, A. Ruiz, J. C. Wolfe, P. Ruchhoeft, E. Svedberg, S. Khizroev, D. Litvinov, *Nanotechnology* **2006**, *17*, 2079.
[24] S. Ikeda, K. Miura, H. Yamamoto, K. Mizunuma, H. Gan, M. Endo, S. Kanai, J. Hayakawa, F. Matsukura, H. Ohno, *Nat. Mater.* **2010**, *9*, 721.
[25] R. Sbiaa, S. Lua, R. Law, H. Meng, R. Lye, H. Tan, *J. Appl. Phys.* **2011**, *109*, 07C707.
[26] J. S. Moodera, L. R. Kinder, T. M. Wong, R. Meservey, *Phys. Rev. Lett.* **1995**, *74*, 3273.
[27] C. Zhou, J. Xu, Y. Wu, *Phys. Rev. Mater.* **2024**, *8*, 024408.
[28] N. Cotón, J. P. Andrés, E. Molina, M. Jaafar, R. Ranchal, *J. Magn. Magn. Mater.* **2023**, *565*, 170246.
[29] A. Castellanos-Gomez, M. Buscema, R. Molenaar, V. Singh, L. Janssen, H. S. Van Der Zant, G. A. Steele, *2D Mater.* **2014**, *1*, 011002.
[30] M. Jaafar, O. Iglesias-Freire, L. Serrano-Ramón, M. R. Ibarra, J. M. de Teresa, A. Asenjo, *Beilstein J. Nanotechnol.* **2011**, *2*, 552.
[31] D. Martinez-Martin, M. Jaafar, R. Perez, J. Gomez-Herrero, A. Asenjo, *Phys. Rev. Lett.* **2010**, *105*, 257203.
[32] M. A. Augustyniak-Jabłokow, K. Tadyszak, R. Strzelczyk, R. Fedaruk, R. Carmieli, *Carbon* **2019**, *152*, 98.
[33] S. Sarma, B. Ghosh, S. C. Ray, H. Wang, T. Mahule, W. Pong, *J. Phys.: Condens. Matter* **2019**, *31*, 135501.
[34] S. Zhou, Y. Wang, Y. Liu, *Magnetochemistry* **2022**, *8*, 159.
[35] C. Felser, G. H. Fecher, B. Balke, *Angew. Chem., Int. Ed.* **2007**, *46*, 668.
[36] Z. He, M. Hassan, H. X. Ju, R. Wang, J. L. Wang, J. F. Chen, J. F. Zhu, J. W. Liu, S. H. Yu, *Nano Res.* **2018**, *11*, 3353.
[37] W. H. Chae, T. Sannicolo, J. C. Grossman, *ACS Appl. Mater. Interfaces* **2020**, *12*, 17909.
[38] Y. Ominato, M. Koshino, *Phys. Rev. B* **2012**, *85*, 165454.
[39] M. Mi, H. Xiao, L. Yu, Y. Zhang, Y. Wang, Q. Cao, Y. Wang, *Materials Today Nano* **2023**, *24*, 100408.
[40] A. Begué, N. Cotón, R. Ranchal, *J. Mater. Chem. C* **2024**, *12*, 10104.
[41] C. Bran, E. Berganza, E. M. Palmero, J. A. Fernández-Roldán, R. Del Real, L. Aballe, M. Foerster, A. Asenjo, A. F. Rodríguez, M. Vazquez, *J. Mater. Chem. C* **2016**, *4*, 978.
[42] W. S. Hummers Jr, R. E. Offeman, *J. Am. Chem. Soc.* **1958**, *80*, 1339.
[43] C. Gómez-Navarro, R. T. Weitz, A. M. Bittner, M. Scolari, A. Mews, M. Burghard, K. Kern, *Nano Lett.* **2007**, *7*, 3499.
[44] I. Horcas, R. Fernández, J. Gomez-Rodriguez, J. Colchero, J. Gómez-Herrero, A. Baro, *Rev. Sci. Instrum.* **2007**, *78*, 013705.
[45] A. Gimeno, P. Ares, I. Horcas, A. Gil, J. M. Gómez-Rodríguez, J. Colchero, J. Gomez-Herrero, *Bioinformatics* **2015**, *31*, 2918.